IEEE Access
Multidisciplinary | Rapid Review | Open Access Journal

Received March 11, 2022, accepted March 31, 2022, date of publication April 5, 2022, date of current version April 14, 2022.

Digital Object Identifier 10.1109/ACCESS.2022.3165049

Multiple Elements MIMO Antenna System With Broadband Operation for 5th Generation Smart Phones

SAAD HASSAN KIANI[1,2], (Graduate Student Member, IEEE), AMJAD IQBAL[3], (Member, IEEE), SAI-WAI WONG[4], (Senior Member, IEEE), HUSEYIN SERIF SAVCI[5], (Senior Member, IEEE), MOHAMMAD ALIBAKHSHIKENARI[6], (Member, IEEE), AND MARIANA DALARSSON[7], (Member, IEEE)

[1]Department of Electrical Engineering, IIC University of Technology, Phnom Penh 121206, Cambodia
[2]Smart Systems Engineering Laboratory, College of Engineering, Prince Sultan University, Riyadh 11586, Saudi Arabia
[3]Institut National de la Recherche Scientifique (INRS), Montreal, QC H5A 1K6, Canada
[4]College of Electronics and Information Engineering, Shenzhen University, Shenzhen 518060, China
[5]Electrical and Electronics Engineering Department, Istanbul Medipol University, 34810 Istanbul, Turkey
[6]Department of Signal Theory and Communications, Universidad Carlos III de Madrid, Leganés, 28911 Madrid, Spain
[7]School of Electrical Engineering and Computer Science, KTH Royal Institute of Technology, 100-44 Stockholm, Sweden

Corresponding authors: Mohammad Alibakhshikenari (mohammad.alibakhshikenari@uc3m.es) and Mariana Dalarsson (mardal@kth.se)

This work was supported by the Universidad Carlos III de Madrid and the European Union's Horizon 2020 Research and Innovation Program through the Marie Sklodowska-Curie Grant 801538.

ABSTRACT In this work, a simple, low-cost, dual wideband sub6GHz Multiple Input Multiple Output (MIMO) antenna system for a smart phone is presented. The antenna system is fabricated using inexpensive and commercially easily available 0.8 mm thick FR4 substrate. The presented system consists of a single main board and two side boards containing eight antennas and feedings. The radiating elements are etched on the side boards to provide space for other electronic components and RF systems and sub systems. The dimensions of the main board and the two side boards are $150 \times 75 \times 0.8$ mm^3 and $150 \times 6 \times 0.8$ mm^3, respectively. The radiating elements are etched on the side substrates and the feeding network is designed on the main board. The proposed system resonates at 3.5 GHz and 5 GHz providing -10 dB bandwidth of 250 MHz (ranges from 3.3 GHz to 3.55 GHz) and 1700 MHz (ranges from 4.2 GHz to 6.2 GHz), respectively. The design and the arrangement of the structure enable pattern diversity and ensures at least -15 dB of isolation between any two given radiating elements. Moreover, various different key performance parameters such as envelope correlation coefficient (ECC), mean effective gain (MEG), channel capacity (CC), specific absorption rate (SAR), gain, and efficiency are also presented. It is found that the peak gain of the system is 5.8 dBi, ECC is lower than 0.015, efficiency ranges between 58% to 78%, peak SAR is 1.28 W/Kg, and the maximum CC is 40.2 bps/Hz within the frequency band of interest. In addition, to further demonstrate the usefulness of such structure as a smart mobile terminal, single and dual hand scenarios are also presented. To validate the concept and the computed results, a prototype is fabricated and measured. It is found that the simulated results are in very good agreement with the measured results. Based on the performance and the measured results, we believe that this structure holds a promising future within the next generation smart mobile phones.

INDEX TERMS Multi-input-multi-output (MIMO), wideband, mutual coupling, envelope correlation coefficient (ECC), pattern diversity, gain.

I. INTRODUCTION

Development of the Fifth Generation (5G) technology is progressing day by day with a demand of high data rate [1]. The increasing demand of high data traffic from the different channels like social media applications, cloud computing, internet, artificial intelligence applications, etc., has set a demanding situation to move towards the 5G technology [2]. Due to structural and performance limitations 4G will not be able to tackle the challenges arising with the passage of the

The associate editor coordinating the review of this manuscript and approving it for publication was Adao Silva.

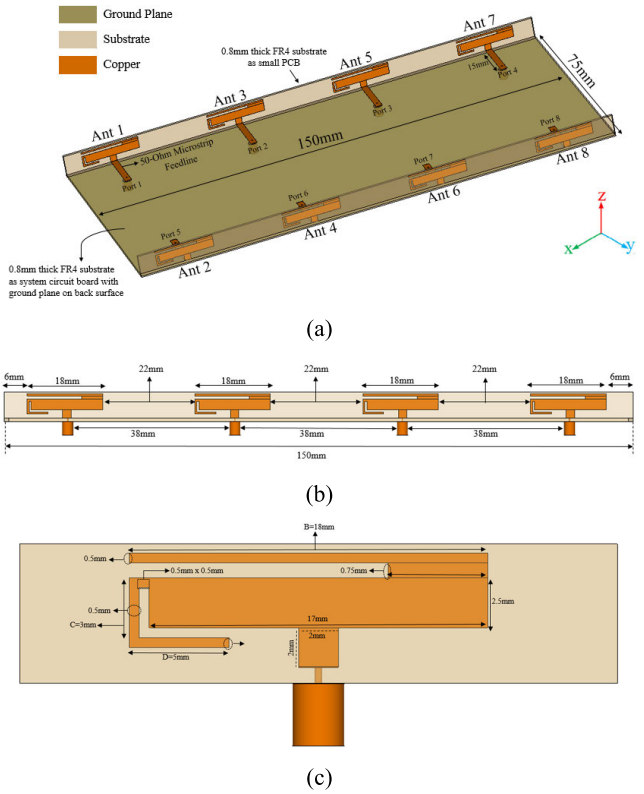

FIGURE 1. The proposed MIMO antenna system. (a): Perspective view. (b): Front view of a side substrate. (c): A single element.

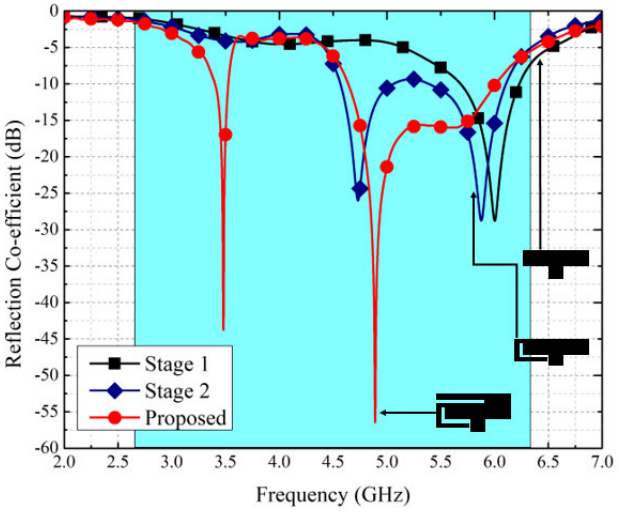

FIGURE 2. Design evolution of proposed wideband antenna.

time in terms of high data rates and bandwidth demand [3]. In addition, low latency is also a challenging requirement for the future era [4]. Therefore, to address such challenges, it is believed that Multiple-Input-Multiple-Output (MIMO) technology can be a better solution to achieve a high data rate requirement by reducing the processing time of data and to improve the transmission rate [1]. Moreover, two portions of the spectrum i.e., Sub-6 GHz and millimeter wave portion of the spectrum are also being considered to upgrade the current technology [5]–[7]. From literature, it is evident that sub 6 GHz band is quite matured in terms of experiments and research conducted [8]. While the millimeter band is still being investigated in terms of experiments and it is believed that more research work is still needed to implement the concepts proved in sub 6 GHz band. But there are several critical challenges which are a hurdle to move ahead with this portion of the spectrum. Some of them are, atmospheric attenuations, cell size, and large number of base stations etc., [9], [10]. Thus, most of countries have implemented a transmission based on the 5G sub 6 GHz portion of the spectrum on initial basis [11]. However, there is still a huge demand to work within this band and standardize the band in terms of technologies and performance of the communication system [12]–[14]. One of the key requirements is to develop antenna such that it maintains its compactness and provide good isolation when the single element is extended to the multi-port configuration [15]–[17]. Furthermore, more than one of the operating bands should be covered to provide multi-band transmission with a reasonable efficiency within the operating band [18]–[20]. Thus, the antenna should also be able to provide multi-functioning to meet the new challenging while maintaining the other standards.

In the last decade, several antennas have been reported to cover the sub 6 GHz operating band [21]–[28]. In [21], dual band antenna with a panel size of 140×70 mm^2 is proposed. The operating bands are 3.4 GHz to 3.6 GHz and 5.4 GHz to 5.6 GHz. The size of the antenna element is 9.6 x 10 mm^2 and the minimum isolation observed within the frequency band is -11 dB. Similarly, another MIMO antenna system with a panel and antenna element size of 150×75 mm^2 and 14.9×4 mm^2, respectively is presented in [22]. The operating bands covered ranges from 3.4-3.6 GHz to 5.1-5.9 GHz while the decoupling level achieved is -12 dB, within the operating band. Moreover, the maximum total efficiency observed is 70%. In [23], a dual band antenna with a panel and antenna element size of 124×74 mm^2 and 6.8×6 mm^2, respectively is presented. The isolation of greater than -15 dB is achieved with a maximum efficiency of more than 70%. Similarly, another dual band antenna with a panel and antenna element size of 130×70 mm^2 and 18×7.7 mm^2, respectively is proposed in [24]. The minimum isolation of -12 dB is achieved with a maximum efficiency of more than 63% within the operating band. In [25], a single band antenna i.e., 3.3 GHz to 5 GHz is proposed. The antenna element size noted is 21.5×6 mm^2. The proposed design is extended to the MIMO configuration with panel size of 150×75 mm^2 while a minimum isolation level of -13 dB is observed. The total efficiency noted is in the range of 30% to 80 %. Another dual band MIMO antenna is presented in [26] which can provide a maximum isolation of -17 dB. However, the total efficiency ranges up to 69%, at maximum. The proposed antenna element size is 10.4×6.8 mm^2 while the MIMO antenna panel size is 150×73 mm^2. The bandwidth achieved is ranging from 3.4 GHz to 3.6 GHz

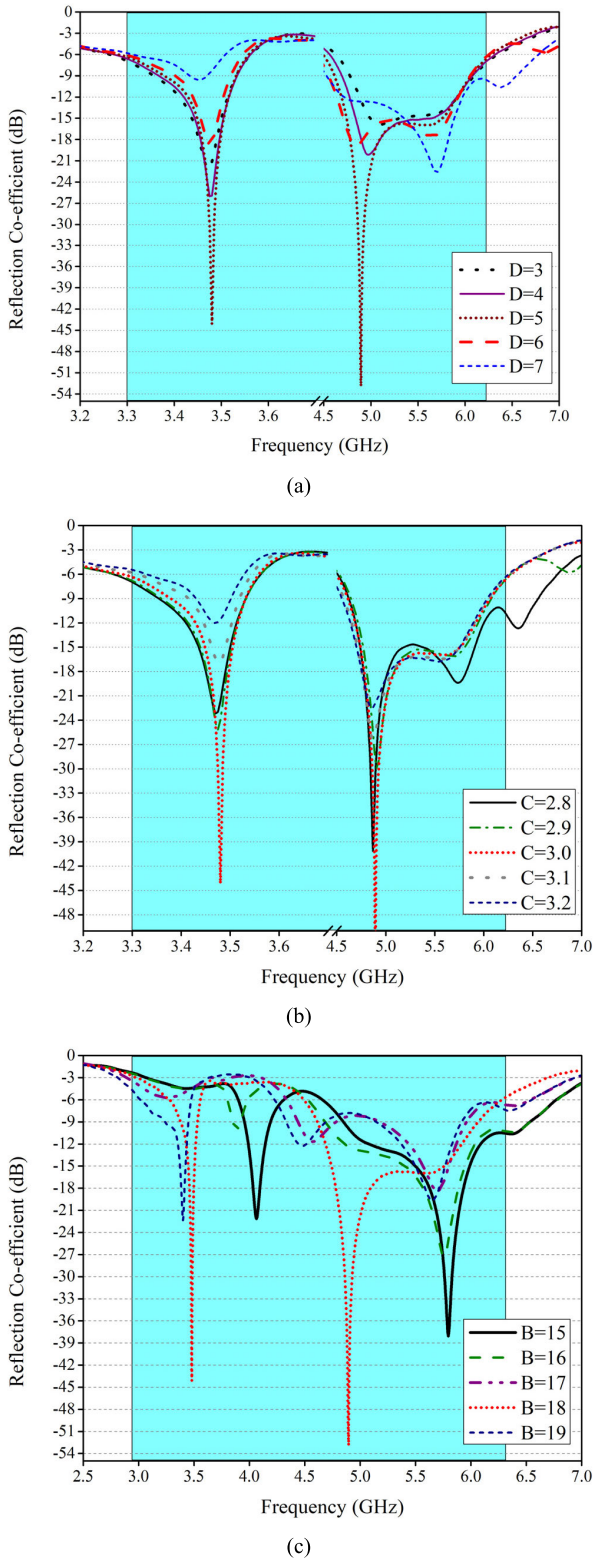

FIGURE 3. Parametric analysis of different variables. (a): Length of the horizontal section of the L-Shaped stub. (b): Length of the vertical section of the L-shaped stub (c): Length of the single stub within the radiating element.

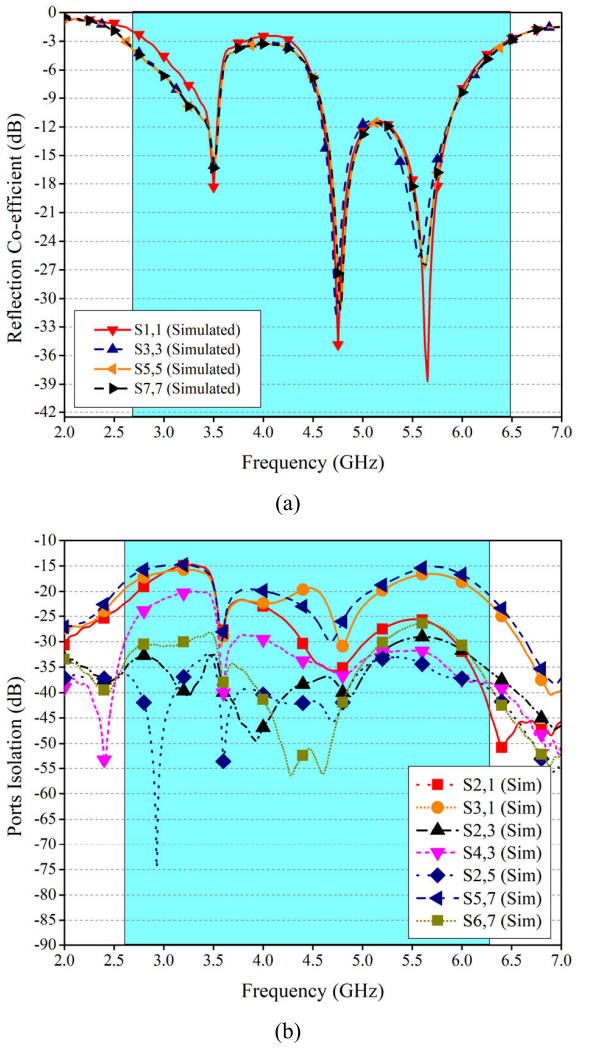

FIGURE 4. Scattering parameters of the proposed system. (a): Return loss of the antennas. (b): Isolation between the ports.

(a) (b)

FIGURE 5. Fabricated prototype. (a): Before joining side substrates. (b): Final form.

and 4.8 GHz to 5 GHz. Similarly, another dual band antenna, capable to operate at 3.2 GHz to 3.8 GHz and 4.7 GHz to 6.2 GHz bandwidths dedicated for 5G sub 6 GHz applications is presented in [27]. The MIMO feature is attained in the

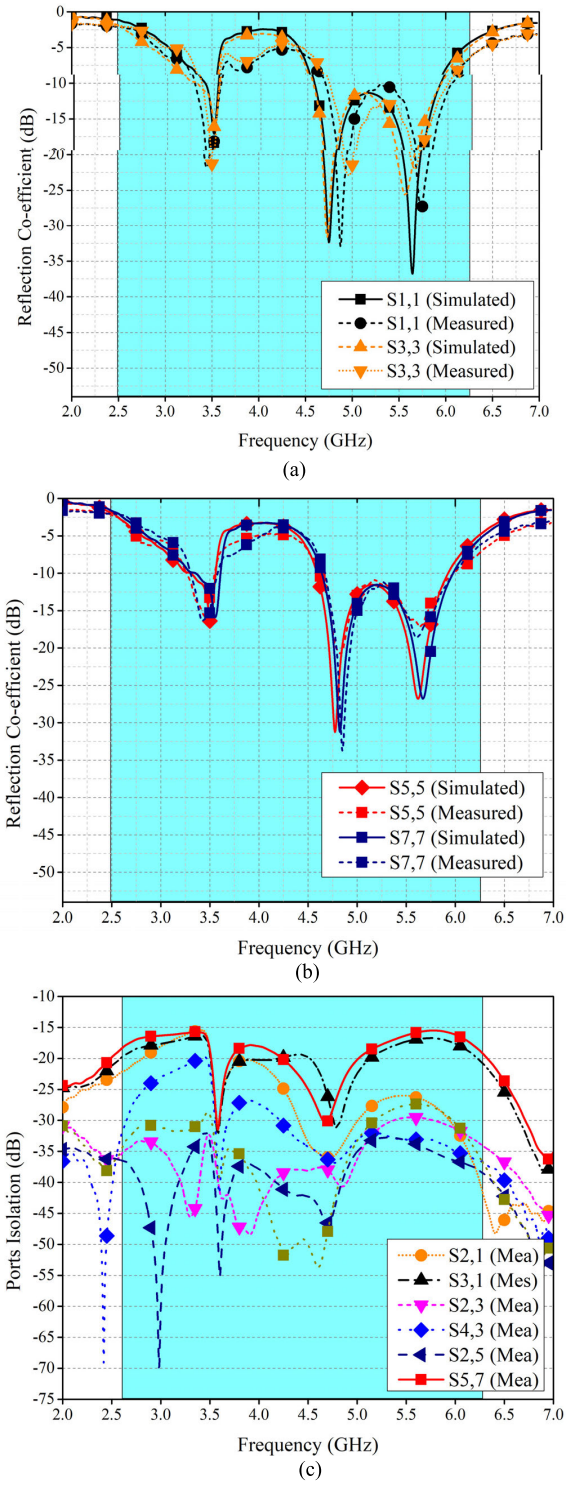

FIGURE 6. Scattering parameters of the proposed system. (a): Simulated and measured return loss of the antennas 1 and 3. (b): Simulated and measured return loss of the antennas 5 and 7 (c) Measured isolation between the ports.

proposed work, but the minimum isolation level is −10 dB within the operating band which is also quite low. The single element size of the proposed radiating element is 15 × 3 mm^2 while the proposed MIMO antenna system itself holds a size

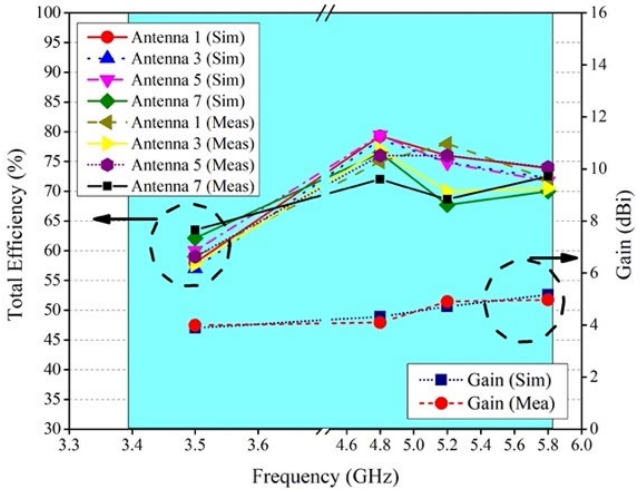

FIGURE 7. Efficiency and gain of the proposed system.

of 150 × 75 mm^2. However, the maximum efficiency of 82% is attained which is sufficient for the 5G sub 6 GHz communication technology. In [28], an antenna covering the 3.4 GHz to 6.0 GHz band is proposed, and a wide-bandwidth response is achieved but only the single band operation is provided in the proposed work. A good isolation level of −18 dB is observed with an efficiency ranging from 40% to 71 %.

From published work in the literature that some of the reported designs have low efficiency, while other works have covered limited number of proposed frequency bands. In addition, it is noted that a few of them adopted MIMO configuration but the achieved isolation level is quite low which makes them not a good fit for the 5G sub 6 GHz applications.

To address these concerns, in this work a simple, low-cost, easy to fabricate and integrate, and dual and wideband compact antenna MIMO antenna system is proposed. The proposed structure is designed on the side boards to provide space for different systems and sub systems. It also enables protection of battery and LCD of shorting if the ground plane is on the same side. In addition, minimum of −15 dB isolation is achieved between any two antenna elements for the whole operating bandwidth.

To demonstrate the contribution and the motivation of this work, a detailed comparison with the recent published works and performance of different key parameters are also presented. Based on the characteristics inherit by this system, performance, and comparison with the literature suggest that it may be used as a potential candidate for 5G mobile terminal.

II. ANTENNA DESIGN

The Figure 1 shows the proposed antenna system. The perspective view is illustrated in Fig. 1a. Similarly, front view of a side substrate and a single element is depicted in Fig. 1b and Fig. 1c, respectively.

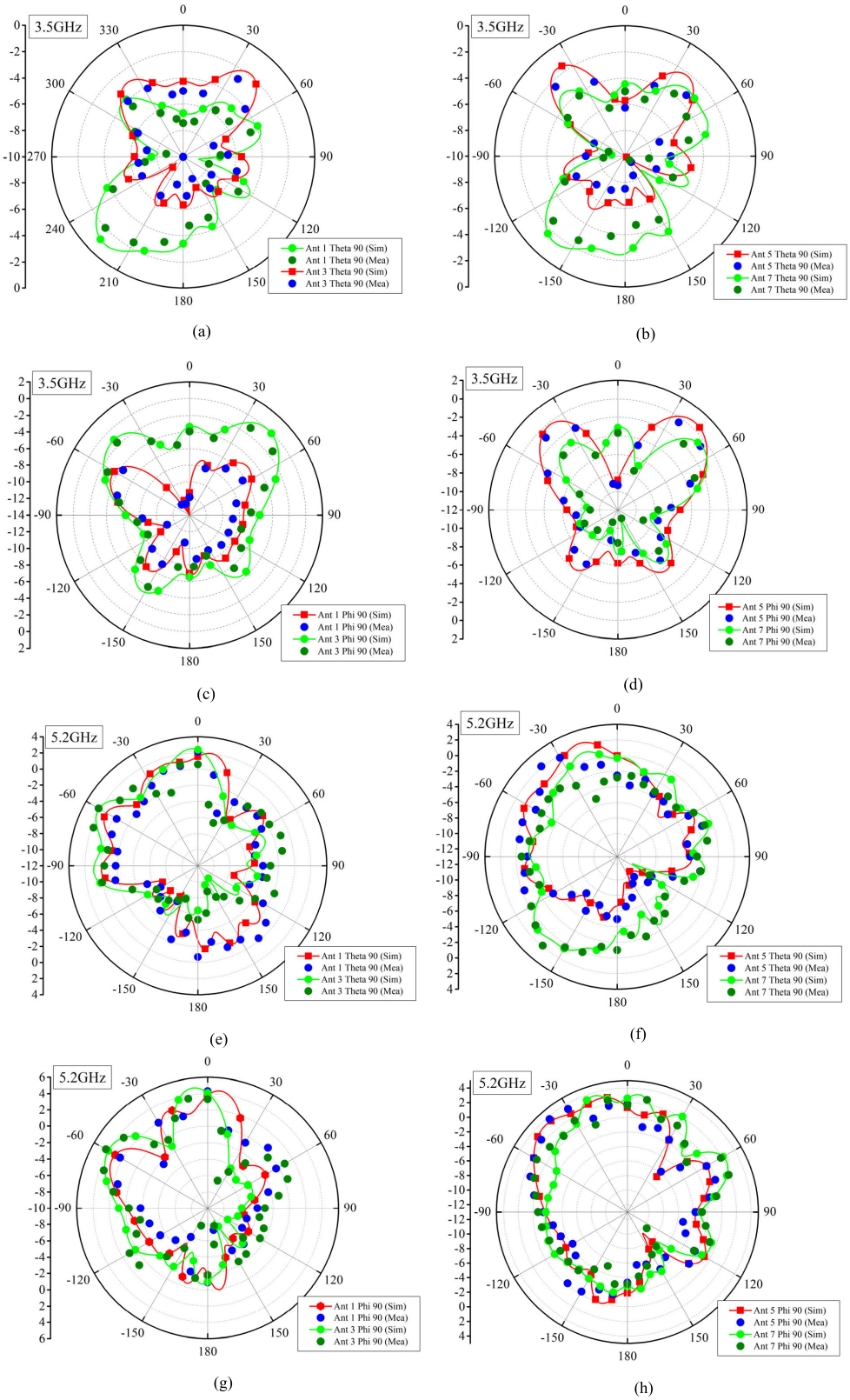

FIGURE 8. Simulated and measured radiation patterns (a) Ant 1 Ant 3 Theta 90 at 3.5GHz (b) Ant 5 Ant 7 Theta 90 at 3.5GHz (c) Ant 1 Ant 3 Phi 90 at 3.5GHz (d) Ant 5 Ant 7 Phi 90 at 3.5GHz (e) Ant 1 Ant 3 Theta 90 at 5.2GHz (f) Ant 5 Ant 7 Theta 90 at 5.2GHz (g) Ant 1 Ant 3 Phi 90 at 5.2GHz (h) Ant 5 Ant 7 Phi 90 at 5.2GHz.

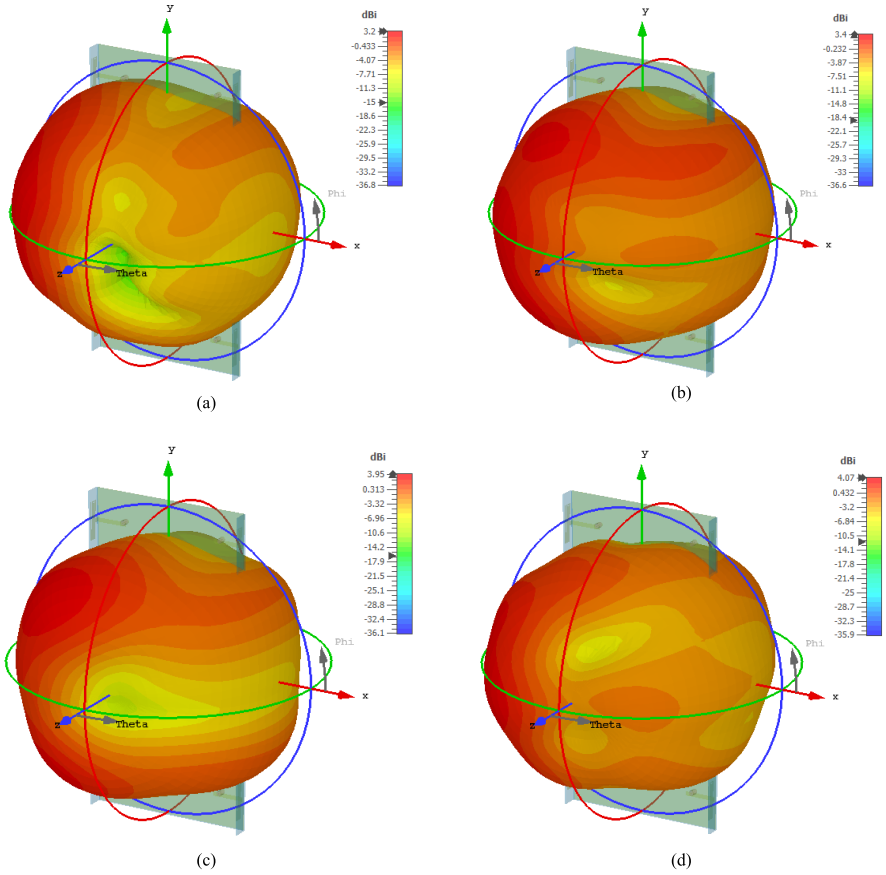

FIGURE 9. 3D Radiation Patterns at 3.5GHz (a) Ant 1 (b) Ant 3 (c) Ant 5 (d) Ant 7.

Figure 1a represents a main board and two side substrates. For both boards, two-sided 0.8 mm thick FR4 substrates are used. The radiating elements are etched on the side substrates, while the microstrip transmission lines are used as feed and the whole system is excited by coaxial cables located on the main substrate. The dielectric constant of the substrate is 4.4, and the loss tangent is 0.03. The total size of the main board and the side substrate is 150×75 mm^2 and 150×6 mm^2, respectively.

On each side-substrate, four antenna elements are designed corresponding to a 1×4 linear array configuration, as illustrated in Fig. 1b. Moreover, a single element along with all dimensions are presented in Fig. 1c. A single element comprises of three rectangular stubs, each element is fed using a microstrip transmission line and a coaxial cable. For details of the size and dimensions, readers are referred to Fig. 1. The presented system is modeled and simulated using a full-wave electromagnetic software Computer Simulation Technology (CST) 2021 using a frequency domain solver and a maximum mesh cell of size $\lambda_0/15$.

Figure 1a represents a main board and two side substrates. For both boards, two-sided 0.8 mm thick FR4 substrates are used. The radiating elements are etched on the side substrates, while the microstrip transmission lines are used as feed and the whole system is excited by coaxial cables located on the main substrate. The dielectric constant of the substrate is 4.4, and the loss tangent is 0.03. The total size of the main board and the side substrate is 150×75 mm^2 and 150×6 mm^2, respectively. On each side-substrate, four antenna elements are designed corresponding to a 1×4 linear array configuration, as illustrated in Fig. 1b. Moreover, a single element along with all dimensions are presented in Fig. 1c.

To understand the working of a single element, it is easy to see that stubs of different widths are added to achieve resonances at different frequencies of interest and then they are joined and optimized to obtain the desired response within required frequency band, as illustrated in Fig. 2. In first stub, a single resonance was obtained central frequency of 6GHz. After inserting second inverted L shape stub, resonance response got wider from 4.2 to 6.2GHz. The third strip generated the lower band response from 3.3 to 3.55GHz. The simulated results show that it is resonating at 3.5 GHz and 5 GHz providing -10 dB bandwidth of 250 MHz (ranges from 3.3 GHz to 3.55 GHz) and 1700 MHz (ranges from 4.5 GHz to 6.2 GHz), respectively. Also, another explanation would be that presented structure is acting like a meander line that not only increase the path of the current but also act as a slow wave antenna that uses the same length occupying less space confining fields in a small region of

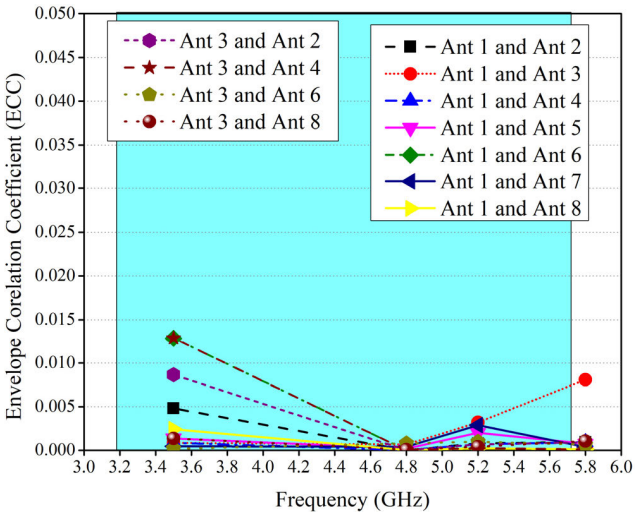

(a)

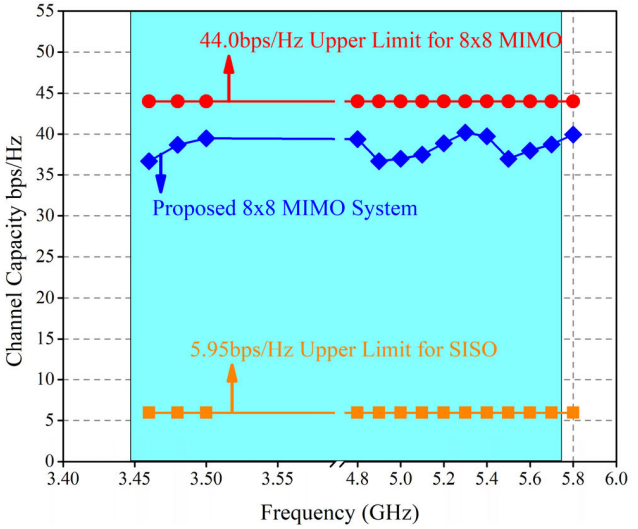

(b)

FIGURE 10. (a) Envelope correlation coefficient. (b) Calculated channel capacity at SNR = 20dB.

18×5.75 mm^2. It is also evident that the prosed antenna element is small and compact allowing space for other communication devices and RF systems and sub-systems. Next, computed, and measured results for the proposed system are presented.

To further presents the working principle of the structure, a parametric analysis of different dimensional parameters is shown in Fig. 3. From Fig. 3, it is evident that the impedance of the antenna changes with changing values at the desired frequency band. For instance, the length of the L-shaped stub (parameter C and D) is influencing the impedance of the radiating element, because the path of the current is lengthened or shorten based on the length. Also, this is due to the fact that each stub is holding a resonant point within the operating bandwidth.

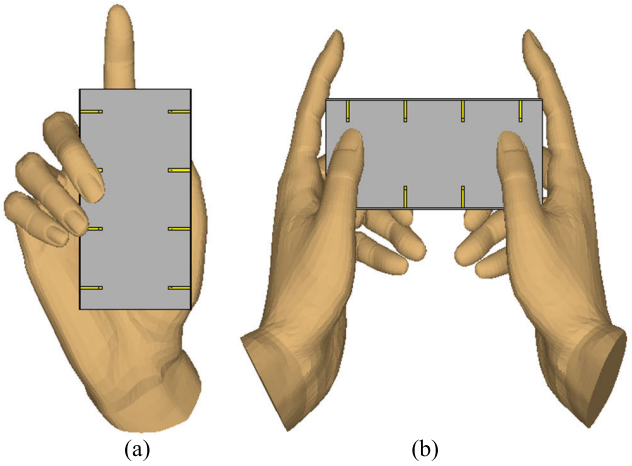

(a) (b)

FIGURE 11. User hands (a) Single hand (b) Two hand.

III. RESULTS AND DISCUSSIONS

The proposed system consists of four radiating elements on each side-substrate. In other words, they are arranged in 1×4 linear array configuration. The edge-to-edge distance between any two radiating elements is 22 mm, while the center-to-center distance is 38 mm. Figure 4 shows the reflection coefficients of different antenna ports and isolation between them. Please note that all antennas have similar resonating response and the isolation between adjacent elements are at least -15 dB, while the elements that are far away for instance, element-1 and element-5 have isolation of -35 dB over the required bandwidth. These attributes inherit by the system ensures pattern diversity and excellent full-duplex communication at a given instant.

Figure 5 shows the fabricated prototype of the antenna. The proposed MIMO antenna array is fabricated using LPFK machine and is tested at in house facility. Figure 6 shows the scattering parameters of fabricated prototype. The measured fabricated scattering parameters are in good agreement as compared to simulated results. The minimum isolation value of -15dB is observed and the reflection coefficient seems to be in agreement as that of simulated results.

Figure 7 represents the total efficiency and the gain of the system. The left y-axis shows the efficiency, while the right y-axis depicts the gain of the system. It can be seen from the figure that gain of the system for the band of interests remains above 4 dBi. Similarly, the efficiency of the system is ranges between 58% to 78%. The efficiency of the antenna elements that are at the corner has better response as compared to the sandwiched elements. This is due to the fact that the corner elements have more free propagation path to radiate. In summary, the efficiency and gain of the system is in very good agreement with the measured results and have peak values of 78% and 5.8 dBi, respectively.

To understand the far-field characteristics of the system, two corner antenna elements (antenna 1 and antenna 5) and two sandwiched (middle) radiating elements (antenna 3 and antenna 7) are studied. For each element two different

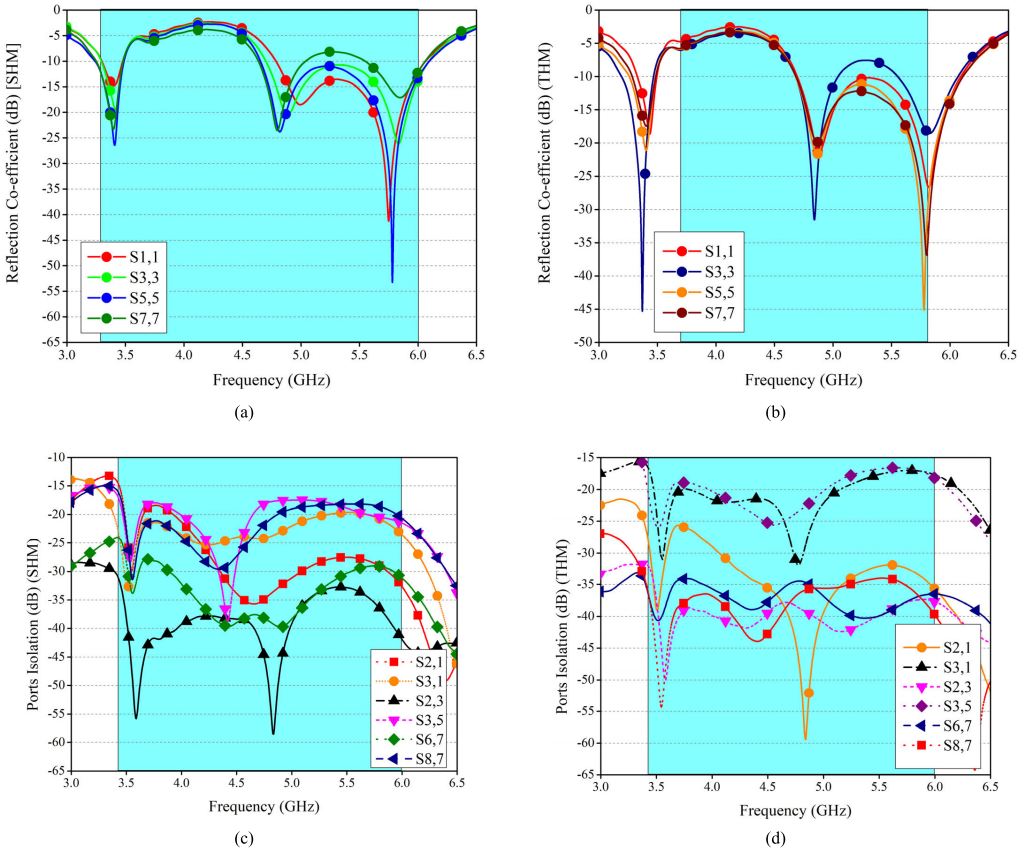

FIGURE 12. S-parameters of the system in the presence of a user's hand. (a): Reflection coefficient-SHM mode. (b): Reflection coefficient-THM mode. (c): Port isolation-SHM mode. (d): Port isolation-THM mode.

frequencies (3.5 GHz and 5.2 GHz) and two different planes i.e., xy- and yz- planes ($\theta = 90^o$ and $\phi = 90^o$, respectively) are discussed. In addition, for each investigation simulated and measured results are compared. Figure 6a and Figure 6b illustrate the radiation characteristics of xy-plane for all four antenna elements. It can be seen that all antennas at 3.5 GHz have peak at $\pm 45^o$ and smaller back lobes. From Fig. 6c and Fig. 6d, far-field characteristics are more prominent at $\pm 45^o$ with a null at 0^o. Similarly, from Figure 6e to Fig. 6h, the patterns are more tilted in space towards -60^o providing directive beams with a smaller back radiation. The radiation attributes of the whole system in the Fig. 8 covers complementary space regions, hence providing pattern diversity characteristics. Similarly, in Figure 9, the 3D radiation patterns at 3.5GHz is given. The 3D radiation patterns of Ant 1, Ant 3, Ant 5 and Ant 7 are shown.

Next, MIMO parameters such as, envelope correlation coefficient (ECC), mean effective gain (MEG), channel capacity (CC), and user hand analysis are investigated. The ECC represents the influence of a radiating element on the performance of other radiating elements within a system. In other words, it measures the interference between the radiating elements. The ECC of the proposed system is given by Fig. 10(a). It is noted that for any given antenna element, it is well lower than 0.015 for the whole operating bands.

TABLE 1. Mean effective gain (MEGs) of proposed antenna system.

Antenna	3.5GHz	4.8GHz	5.2GHz	5.8GHz
1	-4.12	-3.78	-3.59	-3.7
2	-3.09	-3.78	-4.52	-4.1
3	-3.36	-3.85	-3.98	-4.0
4	-3.12	-3.30	-3.51	-3.05
5	-3.71	-3.55	-3.62	-4.19
6	-3.65	-3.56	-3.77	-3.98
7	-3.88	-3.25	-3.15	-3.05
8	-3.11	-3.13	-3.45	-3.23

Similarly, MEG indicates the gain of the system in a multipath environment. The calculated MEG is less than 1 dB for both desired frequency bands, as shown in Table-1. The channel capacity of the proposed MIMO Antenna system is calculated by averaging the 10,000 Rayleigh fading realization with a

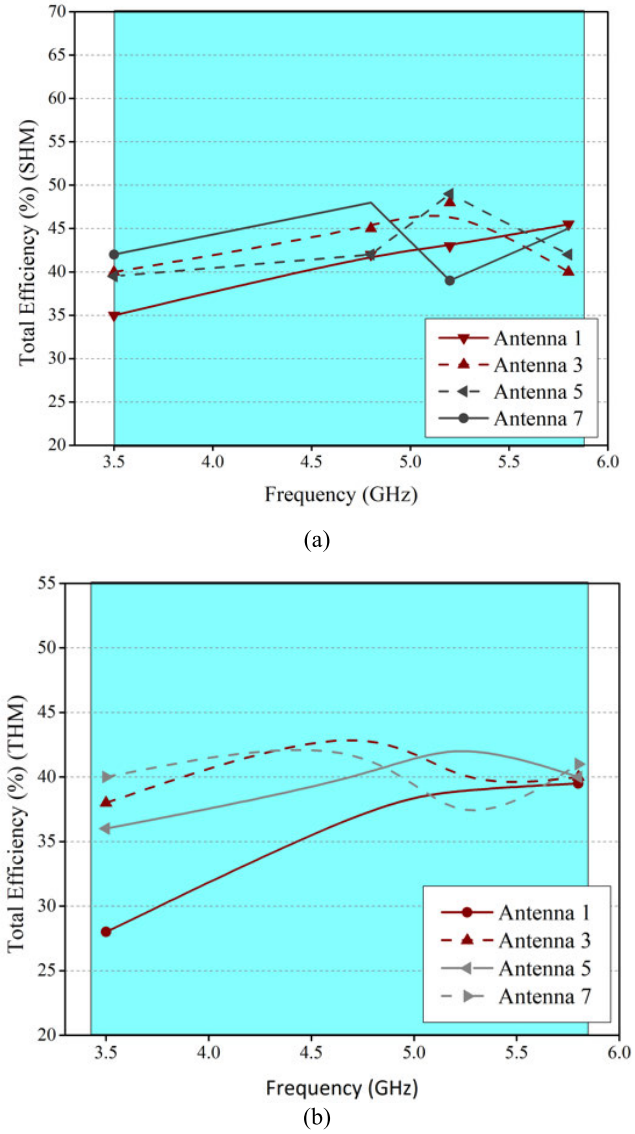

FIGURE 13. Total efficiency of the proposed system in the presence of a user's hand. (a): SHM. (b): THM.

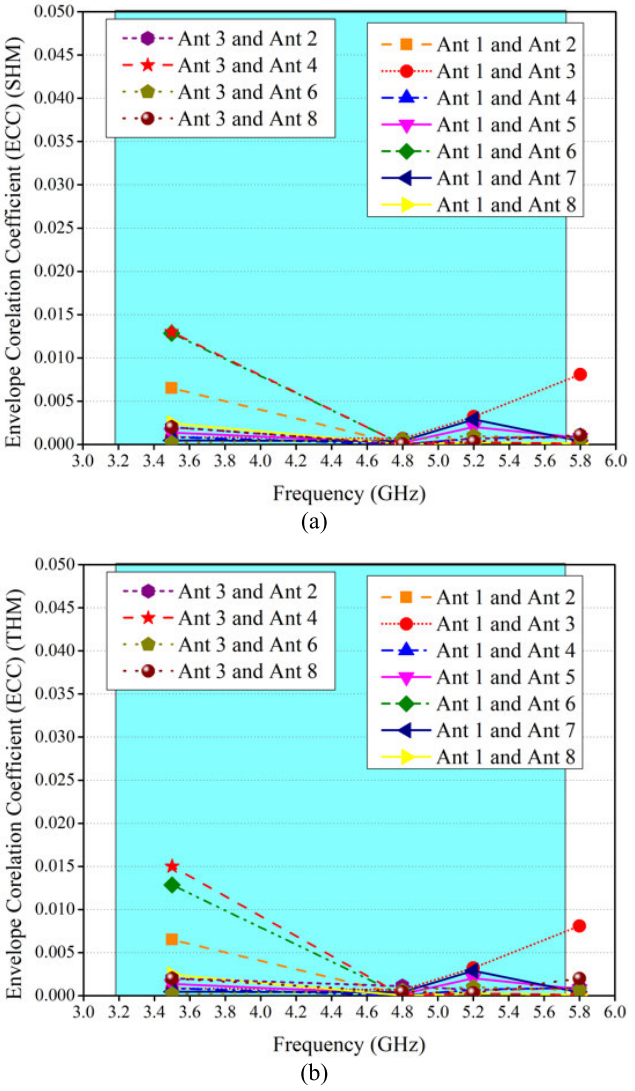

FIGURE 14. ECC of the proposed system in the presence of a user's hand. (a): SHM. (b): THM.

reference signal to noise ratio (SNR) of 20 dB. The peak channel capacity is found to be at 40.2 bps/Hz which is close to an ideal eight-element antenna array capacity of 46 bps/Hz, as illustrated in Fig. 10(b).

IV. USER HAND ANALYSIS

As discussed earlier, the proposed system is designed with aim to cover desired sub6GHz 5G bands for a smart phone terminal. Therefore, impact of user's hand needs to be investigated. Here, the influence of chatting (single-hand) and gaming (two-hand), as shown in Fig. 11, are discussed. Three key performance parameters, S-parameters, efficiency, and ECC for both hand modes are discussed.

First, a hand model is imported from a CST library into the simulation file and is characterized by the properties given by [13]. From literature, it is well understood that the effective permittivity of a human hand varies between 28 and 32 with an average electric conductivity range between 0.7 S/m to 0.9 S/m. Therefore, in this study, the hand model is characterized by permittivity of 29 and electric conductivity of 0.9 S/m. The influence of a user's hand over the scattering parameters of the system is given by Fig. 12. For both modes i.e., SHM and THM, the impedance changes for both frequency bands. This shift in the impedance is attributed to the dielectric loading of the 9system. Please note that the antenna elements which are in close contact with the hand (antenna 7 and antenna 3) have slightly different characteristics as compared with other radiating elements. Similarly, the isolation of the system for any two antenna elements is well below −15 dB that ensures less interference between the elements. The scattering parameters (reflection coefficients and isolation between the ports) are shown in Fig. 12.

Next, other performance metrics of the system in the presence of a user's hand i.e., efficiency and ECC are

TABLE 2. Comparison table of the proposed MIMO antenna.

Reference	Frequency (GHz)	Board Size	Antenna Element (L x W)	Isolation (dB)	Efficiency (%)	ECC	CC
[21]	3.4-3.6/ 5.4-5.6	140 x 70	9.6 x 10	-11	51-59/62-80	<0.1	36
[22]	3.4-3.6/ 5.1-5.9	150 x 75	14.9 x 4	-12	60-65/58-70	<0.2	40
[23]	2.4-2.7/3.3-3.6	124 x 74	6.8 x 6	>15	60-80/55-70	<0.12	35
[24]	1.6-3.7/4.1-6.1	130 x 70	18 x 7.7	-12	22-58/50-63	N/A	N/A
[25]	3.3-5.0	150 x 75	21.5 x 6	-13	30-80	0.1	35.5
[26]	3.4-3.6/4.8-5.0	150 x 73	10.4 x 6.8	-17.5	50-65/50-69	<0.15	18.3
[27]	3.2-3.8/4.7-6.2	150 x 75	15 x 3	-10.5	60-85/42-82	0.12	37.6
[28]	3.3-6.0	150 x 75	17 X 5.7	-18	40-71	0.1	N/A
Proposed	3.1-3.6/4.4-6.1	150 x 75	5.77 x 18	-18.5	50-65/65-75	<0.1	40.2

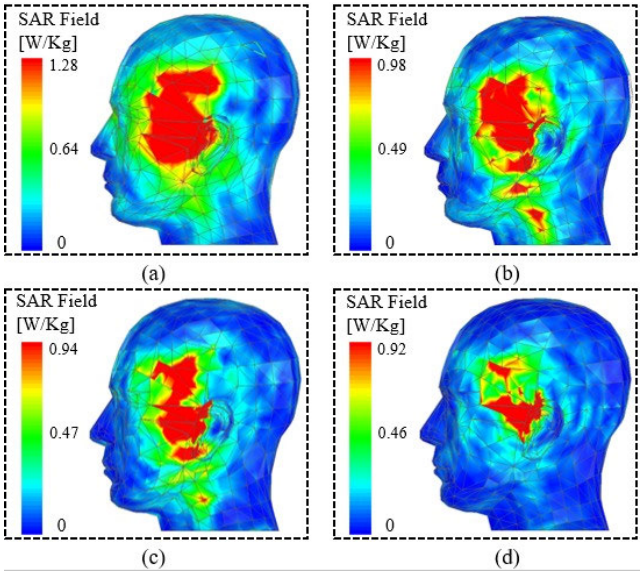

FIGURE 15. SAR of the proposed system. (a)3.5GHz(b)4.8 GHz (c) 5.2GHz (d) 5.8GHz.

investigated. The motive here is to present the impact of a scenario if such system is sued as a mobile terminal. For both hand modes the efficiency is degraded specially for the antenna elements which are in a close proximity of the hand, which was expected, as shown in Fig. 13. The reason for the loss in the efficiency is that most of the power is now absorbed by the hand. It is worthy to mention that for any given mode and a radiating element, ECC is well below 0.015 which is in accordance with the MIMO performance standards, as depicted in Fig. 14.

Since the motivation of this work is to present a low-cost, compact, and efficient mobile terminal. Therefore, it is necessary to study the impact of such system over the health of a human, especially when it is in a working mode i.e., uplink and downlink scenarios. To study this, Specific absorption rate (SAR) is the computed. SAR is usually computed to measure the impact of intensity of the backward radiation of a radiating system on per unit mass of the human body. According to the standards, the SAR should be less than 1.6 W/Kg for a 1-g tissue and 2 W/Kg for 10-g tissue. To calculate the SAR in the simulation environment, the system was placed at 2 mm from a realistic human head. The human head is imported from a CST library with a well-known described property. Each unit of the antenna was powered with an input power of 25 mW, thus the total input power of 200 mW was supplied to the antenna units. Fig. 14 shows the SAR results of the antenna for 1-g tissue. The peak SAR value of 1.28 W/Kg was observed for the desired frequency bands, as shown in Figure. 13. Therefore, on can conclude that the proposed antenna is safe for operations in the vicinity of a human body.

To further demonstrate that the proposed work is better in design and the performance, a detailed comparison of this work with the available works are conducted and illustrated in Table 2. It is worthy to mention that based on different analysis, investigation, and studies, we are confident that the proposed model has potential to be a useful MIMO system for future 5G smart mobile terminals.

V. CONCLUSION

In this work, a simple, low-cost, easy to fabricate and integrate, and dual wideband sub 10 GHz Multiple Input Multiple Output (MIMO) antenna system for a smart phone is presented. The antenna system is fabricated on a 0.8 mm thick FR4 substrate with the dimensions of the main board and the two side boards are $150 \times 75 \times 0.8$ mm^3 and $150 \times 6 \times 0.8$ mm^3, respectively. The radiating elements are etched on the side boards to provide space for other electronic components and RF systems and sub systems. The proposed system resonates at 3.5 GHz and 5 GHz providing -10 dB bandwidth of 250 MHz (ranges from 3.3 GHz to 3.55 GHz) and 1700 MHz (ranges from 4.2 GHz to 6.2 GHz), respectively with a minimum isolation of at least -15 dB between any two given elements. It is found that the peak gain of the system is 5.8 dBi, ECC is lower than 0.015, efficiency

ranges between 58% to 78%, peak SAR is 1.28 W/Kg, and the maximum CCL is 40.2 bps/Hz within the frequency band of interest. In addition, to further demonstrate the usefulness of such structure as a smart mobile terminal, influence of a user's hand for two different modes i.e., chatting and gaming are also presented. A brief literature review and comparison of this work with other published works is also presented. To validate the concept and the computed results, a prototype is fabricated and measured. It is found that the simulated results for various key performance parameters are in very good agreement with the measured results. Based on the performance and the measured results, we believe that this structure holds a promising future within the next generation smart mobile phones.

REFERENCES

[1] A. Desai, C. D. Bui, J. Patel, T. Upadhyaya, G. Byun, and T. K. Nguyen, "Compact wideband four element optically transparent MIMO antenna for mm-wave 5G applications," *IEEE Access*, vol. 8, pp. 194206–194217, 2020.

[2] M. Ikram, N. Nguyen-Trong, and A. Abbosh, "Hybrid antenna using open-ended slot for integrated 4G/5G mobile application," *IEEE Antennas Wireless Propag. Lett.*, vol. 19, no. 4, pp. 710–714, Apr. 2020, doi: 10.1109/LAWP.2020.2978181.

[3] M. Ikram, N. Nguyen-Trong, and A. M. Abbosh, "Common-aperture sub-6 GHz and millimeter-wave 5G antenna system," *IEEE Access*, vol. 8, pp. 199415–199423, 2020, doi: 10.1109/ACCESS.2020.3034887.

[4] M. Ikram, E. A. Abbas, N. Nguyen-Trong, K. H. Sayidmarie, and A. Abbosh, "Integrated frequency-reconfigurable slot antenna and connected slot antenna array for 4G and 5G mobile handsets," *IEEE Trans. Antennas Propag.*, vol. 67, no. 12, pp. 7225–7233, Dec. 2019, doi: 10.1109/TAP.2019.2930119.

[5] N. Hussain, W. A. Awan, W. Ali, S. I. Naqvi, A. Zaidi, and T. T. Le, "Compact wideband patch antenna and its MIMO configuration for 28 GHz applications," *AEU-Int. J. Electron. Commun.*, vol. 132, Apr. 2021, Art. no. 153612.

[6] S. H. Kiani, A. Altaf, M. R. Anjum, S. Afridi, Z. A. Arain, S. Anwar, S. Khan, M. Alibakhshikenari, A. Lalbakhsh, M. A. Khan, R. A. Abd-Alhameed, and E. Limiti, "MIMO antenna system for modern 5G handheld devices with healthcare and high rate delivery," *Sensors*, vol. 21, no. 21, p. 7415, Nov. 2021.

[7] S. H. Kiani, A. Altaf, M. Abdullah, F. Muhammad, N. Shoaib, M. R. Anjum, R. Damaševičius, and T. Blažauskas, "Eight element side edged framed MIMO antenna array for future 5G smart phones," *Micromachines*, vol. 11, no. 11, p. 956, 2020.

[8] Z. Qin, W. Geyi, M. Zhang, and J. Wang, "Printed eight-element MIMO system for compact and thin 5G mobile handest," *Electron. Lett.*, vol. 52, no. 6, pp. 416–418, 2016.

[9] M. Abdullah, S. H. Kiani, and A. Iqbal, "Eight element multiple-input multiple-output (MIMO) antenna for 5G mobile applications," *IEEE Access*, vol. 7, pp. 134488–134495, 2019.

[10] S.-Y. Lin and H.-R. Huang, "Ultra-wideband MIMO antenna with enhanced isolation," *Microw. Opt. Technol. Lett.*, vol. 51, no. 2, pp. 570–573, Feb. 2009.

[11] M. Abdullah, S. H. Kiani, L. F. Abdulrazak, A. Iqbal, M. A. Bashir, S. Khan, and S. Kim, "High-performance multiple-input multiple-output antenna system for 5G mobile terminals," *Electronics*, vol. 8, no. 10, p. 1090, Sep. 2019.

[12] M. Yang and J. Zhou, "A compact pattern diversity MIMO antenna with enhanced bandwidth and high-isolation characteristics for WLAN/5G/WiFi applications," *Microw. Opt. Technol. Lett.*, vol. 62, no. 6, pp. 2353–2364, 2020.

[13] M. S. Khan, A.-D. Capobianco, M. F. Shafique, B. Ijaz, A. Naqvi, and B. D. Braaten, "Isolation enhancement of a wideband MIMO antenna using floating parasitic elements," *Microw. Opt. Technol. Lett.*, vol. 57, no. 7, pp. 1677–1682, 2015.

[14] Z. Xu and C. Deng, "High-isolated MIMO antenna design based on pattern diversity for 5G mobile terminals," *IEEE Antennas Wireless Propag. Lett.*, vol. 19, no. 3, pp. 467–471, Mar. 2020.

[15] L. Yang and T. Li, "Box-folded four-element MIMO antenna system for LTE handsets," *Electron. Lett.*, vol. 51, no. 6, pp. 440–441, 2015.

[16] B. Yang, M. Chen, and L. Li, "Design of a four-element WLAN/LTE/UWB MIMO antenna using half-slot structure," *AEU-Int. J. Electron. Commun.*, vol. 93, pp. 354–359, Sep. 2018.

[17] R. K. Jaiswal, K. Kumari, A. K. Ojha, and K. V. Srivastava, "Five-port MIMO antenna for n79-5G band with improved isolation by diversity and decoupling techniques," *J. Electromagn. Waves Appl.*, vol. 36, no. 4, pp. 542–556, Mar. 2022.

[18] M. Y. Muhsin, A. J. Salim, and J. K. Ali, "An eight-element MIMO antenna system for 5G mobile handsets," in *Proc. Int. Symp. Netw., Comput. Commun. (ISNCC)*, Oct. 2021, pp. 1–4.

[19] M. S. Sharawi, "Current misuses and future prospects for printed multiple-input, multiple-output antenna systems [wireless corner]," *IEEE Antennas Propag. Mag.*, vol. 59, no. 2, pp. 162–170, Apr. 2017.

[20] B. BharathiDevi and J. Kumar, "Small frequency range discrete bandwidth tunable multiband MIMO antenna for radio/LTE/ISM-2.4 GHz band applications," *AEU-Int. J. Electron. Commun.*, vol. 144, Feb. 2022, Art. no. 154060.

[21] J. Li, X. Zhang, Z. Wang, X. Chen, J. Chen, Y. Li, and A. Zhang, "Dual-band eight-antenna array design for MIMO applications in 5G mobile terminals," *IEEE Access*, vol. 7, pp. 71636–71644, 2019.

[22] H. Zou, Y. X. Li, C.-Y.-D. Sim, and G. L. Yang, "Design of 8×8 dual-band MIMO antenna array for 5G smartphone applications," *Int. J. RF Microw. Comput.-Aided Eng.*, vol. 28, no. 9, Nov. 2018, Art. no. e21420.

[23] W. Jiang, Y. Cui, B. Liu, W. Hu, and Y. Xi, "A dual-band MIMO antenna with enhanced isolation for 5G smartphone applications," *IEEE Access*, vol. 7, pp. 112554–112563, 2019.

[24] J. Duan, K. Xu, X. Li, S. Chen, P. Zhao, and G. Wang, "Dual-band and enhanced-isolation MIMO antenna with L-shaped meta-rim extended ground stubs for 5G mobile handsets," *Int. J. RF Microw. Comput.-Aided Eng.*, vol. 29, no. 8, 2019, Art. no. e21776.

[25] A. Zhao and Z. Ren, "Wideband MIMO antenna systems based on coupled-loop antenna for 5G N77/N78/N79 applications in mobile terminals," *IEEE Access*, vol. 7, pp. 93761–93771, 2019.

[26] Z. Ren and A. Zhao, "Dual-band MIMO antenna with compact self-decoupled antenna pairs for 5G mobile applications," *IEEE Access*, vol. 7, pp. 82288–82296, 2019.

[27] H. Wang, R. Zhang, Y. Luo, and G. Yang, "Compact eight-element antenna array for triple-band MIMO operation in 5G mobile terminals," *IEEE Access*, vol. 8, pp. 19433–19449, 2020.

[28] X.-T. Yuan, W. He, K.-D. Hong, C.-Z. Han, Z. Chen, and T. Yuan, "Ultra-wideband MIMO antenna system with high element-isolation for 5G smartphone application," *IEEE Access*, vol. 8, pp. 56281–56289, 2020.

SAAD HASSAN KIANI (Graduate Student Member, IEEE) received the bachelor's degree in electrical engineering (telecommunication) from the City University of Science and Information Technology (CUSIT), in 2014, and the Masters of Science degree in electrical engineering from Iqra National University (IN), Peshawar, Pakistan, in 2018. He is currently pursuing the Ph.D. degree with the IIC University of Technology, Cambodia. He worked as a Lecturer with the CUSIT, and as an Adjunct Faculty with IN. His research interests include MIMO antenna designs, 5G antennas, mmwave antennas, isolation enhancement among MIMO antenna elements, origami and kirigami antennas.

AMJAD IQBAL (Member, IEEE) received the B.S. degree in electrical engineering from COMSATS University, Islamabad, Pakistan, in 2016, and the M.S. degree in electrical engineering from the Department of Electrical Engineering, CECOS University of IT and Emerging Science, Peshawar, Pakistan, in 2018. He worked as a Laboratory Engineer with the Department of Electrical Engineering, CECOS University, from 2016 to 2018. He is currently working as a Graduate Researcher with the Faculty of Engineering, Multimedia University, Cyberjaya, Malaysia. His research interests include printed antennas, flexible antennas, implantable antennas, MIMO antennas, dielectric resonator antennas, wireless power transfer, and synthesis of microwave components.

SAI-WAI WONG (Senior Member, IEEE) received the B.S. degree in electronic engineering from The Hong Kong University of Science and Technology, Hong Kong, in 2003, and the M.Sc. and Ph.D. degrees in communication engineering from Nanyang Technological University, Singapore, in 2006 and 2009, respectively. From July 2003 to July 2005, he was an Electronic Engineer to lead an Electronic Engineering Department in China with two Hong Kong manufacturing companies. From May 2009 to October 2010, he was a Research Fellow with the A*STAR Institute for Infocomm Research, Singapore. Since 2010, he has been an Associate Professor and later become a Full Professor with the School of Electronic and Information Engineering, South China University of Technology, Guangzhou, China. From July 2016 to September 2016, he was a Visiting Professor with the City University of Hong Kong, Hong Kong. Since 2017, he has been a Full Professor with the College of Electronics and Information Engineering, Shenzhen University, Shenzhen, China. He has authored or coauthored more than 200 papers in international journals and conference proceedings. His current research interests include RF/microwave circuit and antenna design. He was a recipient of the New Century Excellent Talents in University awarded by the Ministry of Education of China in 2013 and the Shenzhen Overseas High-Caliber Personnel Level C in 2018.

HUSEYIN SERIF SAVCI (Senior Member, IEEE) received the B.Sc. degree in electronics and communication engineering from Yıldız Technical University, in 2001, and the M.Sc. and Ph.D. degrees in electrical engineering from Syracuse University, Syracuse, NY, USA, in 2005 and 2008, respectively. From 2008 to 2013, he was with Skyworks Solutions Inc., Cedar Rapids, IA, USA, as a Senior RFIC Design Engineer. From 2013 to 2020, he worked with Hittite Microwave Corporation, Chelmsford Massachusetts and Analog Devices Inc., Istanbul, Turkey, as a Principal Design Engineer where he designed many RFIC and MMIC products on SOI, GaN, and GaAs technologies for test and measurement, mm-wave and sub-6GHz cellular infrastructure and ADEF applications. In 2020, he joined the Department of Electrical and Electronics Engineering, Istanbul Medipol University, Istanbul, as an Assistant Professor. His research interests include design and modeling of RF and microwave integrated circuits, devices, systems, and antennas.

MOHAMMAD ALIBAKHSHIKENARI (Member, IEEE) was born in Mazandaran, Iran, in February 1988. He received the Ph.D. degree (Hons.) with European Label in electronic engineering from the University of Rome "Tor Vergata," Italy, in February 2020. He was a Ph.D. Visiting Researcher with the Chalmers University of Technology, Sweden, in 2018. His training during the Ph.D. included a research stage with Swedish company Gap Waves AB. He is currently with the Department of Signal Theory and Communications, Universidad Carlos III de Madrid, Spain, as a Principal Investigator of the CONEX-Plus Talent Training Program and Marie Sklodowska-Curie Actions. He is also a Lecturer of the Electromagnetic Systems and Electromagnetic Laboratory, Department of Signal Theory and Communications. His research interests include electromagnetic systems, antennas and wave-propagations, metamaterials and metasurfaces, synthetic aperture radars (SAR), multiple-input multiple-output (MIMO) systems, RFID tag antennas, substrate integrated waveguides (SIWs), impedance matching circuits, microwave components, millimeter-waves and terahertz integrated circuits, gap waveguide technology, beamforming matrixes, and reconfigurable intelligent surfaces (RIS). The above research lines have produced more than 150 publications on international journals, presentations within international conferences, and book chapters with a total number of the citations more than 2700 and H-index of 36. He was a recipient of the three years research grant funded by the Universidad Carlos III de Madrid and the European Union's Horizon 2020 Research and Innovation Program under the Marie Sklodowska-Curie Grant 801538 started in July 2021, the two years research grant funded by the University of Rome "Tor Vergata" started in November 2019, the three years Ph.D. Scholarship funded by the University of Rome "Tor Vergata" started in November 2016, and the two Young Engineer Awards of the 47th and 48th European Microwave Conference held in Nuremberg, Germany, in 2017, and in Madrid, Spain, in 2018, respectively. His research article entitled "High-Gain Metasurface in Polyimide On-Chip Antenna Based on CRLH-TL for Sub Terahertz Integrated Circuits" published in Scientific Reports was awarded as the Best Month Paper at the University of Bradford in April 2020. He is serving as an Associate Editor for *IET Journal of Engineering* and *International Journal of Antennas and Propagation*. He also acts as a referee in several highly reputed journals and international conferences.

MARIANA DALARSSON (Member, IEEE) received the M.Sc. degree in physics and the Ph.D. degree in electromagnetic theory from the KTH Royal Institute of Technology, Stockholm, Sweden, in 2010 and 2016, respectively, and the Docent degree from Linnaeus University, Växjö, Sweden, in 2019. During 2016–2019, she was a Postdoctoral Researcher with the Group of Waves, Signals and Systems, Linnaeus University. From 2019 to 2020, she was an Assistant Professor at the Department of Electrical and Information Technology, Lund University, Lund, Sweden. She is currently an Assistant Professor at the KTH Royal Institute of Technology, Stockholm, Sweden. She is the author of more than 60 scientific publications, including 25 journal articles and one book. Her research interests include electromagnetic scattering and absorption, inverse problems, electromagnetics of stratified media, double-negative metamaterials, and mathematical physics. She is also mainly pursuing research as a PI within her own project grant "Waveguide Theory for Artificial Materials and Plasmonics" awarded by the Swedish Research Council. She is the winner of multiple teaching and research awards, including the L'Oréal-Unesco For Women in Science Sweden Award in 2021. She received the Honorary Grant given to the Best Graduate of the Year of her M.Sc. program, in 2011. She is also the Second Youngest Woman ever to be awarded a Ph.D. degree from KTH.